Supporting Information

Bougarne et al. 10.1073/pnas.0806742106

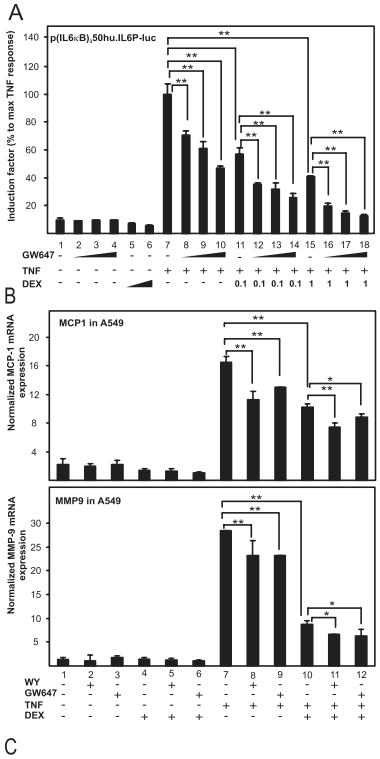

C

Genbank	Acronym	Gene	DMSO vs DEX	DMSO vs DEX+WY
AF065933	Ccl2	chemokine (C–C motif) ligand 2	-2,06	-3,67
AF099052	Ccl20	chemokine (C–C motif) ligand 20	-1,66	-2,43
NM_008176	Cxcl1	chemokine (C–X–C motif) ligand 1	-1,84	-2,86
NM_009140	Cxcl2	chemokine (C–X–C motif) ligand 2	-1,88	-2,64
BB829808	Cxcl3	chemokine (C–X–C motif) ligand 3	-6,14	-8,18
BB250384	VCAM1	vascular cell adhesion molecule 1	-3,37	-4,28

Fig. S1. PPARα and GRα cooperate to inhibit NF-κB-driven gene expression. (*A*) The additive antiinflammatory effect of dexamethasone (DEX) and peroxisome proliferator-activated receptor (PPAR) agonists converges on NF-κB. The figure shows that GW647 and DEX can separately mediate the inhibition of TNF-induced gene expression in a dose-responsive manner (lanes 8–10 and lanes 11 and 15 compared with lane 7) in L929sA cells, stably transfected with p(IL6κB)$_3$50hu.IL6P-luc+, an NF-κB-dependent recombinant promoter construct. The simultaneous activation of PPARα and glucocorticoid receptor α (GRα) (lanes 12–14 compared with lane 11 and lanes 16–18, compared with lane 15) results in a clear additive repression of TNF-induced NF-κB-driven promoter activity. L929sA cells with stably integrated p(IL6κB)$_3$50hu.IL6P-luc+ were preincubated with solvent, DEX (1 or 0.1 μM), GW647 (1, 0.5, or 0.25 μM) or various combinations thereof, for 1 h, before TNF (2,000 units/mL) was added, where indicated, for 6 h. Cell lysates were assayed for luc activities and normalized with β-gal activities. Promoter activities are expressed as relative induction factor calculated as percentage of maximal TNF response. Results are shown $\pm$ SD. **, $P < 0.01$. (*B*) PPARα agonists inhibit mRNA expression of inflammatory markers in A549 cells. The results obtained for IL-6 in L929sA were confirmed in A549 cells at the mRNA level, via QPCR analysis, for other inflammatory markers, namely monocyte chemoattractant protein (MCP)-1 and matrix metalloproteinase (MMP)-9. PPARα agonists are able to enhance the glucocorticoid (GC)-mediated inhibition of TNF up-regulated mRNA levels of MCP-1 and MMP-9, further supporting the general character of our findings. Results are shown $\pm$ SD. *, $P < 0.05$; **, $P < 0.01$. A549 cells were treated with solvent, DEX (1 μM), GW647 (500 nM), or WY (10 μM) or various combinations for 8 h. mRNA was isolated and reverse transcribed, and cDNA was subjected either to SYBR Green quantitative PCR (QPCR) with primers to detect MCP-1 or MMP-9. The sequences of used primer pairs are available upon request. QPCR measurements were performed in triplicate. QPCR results, normalized to expression of household genes, are shown $\pm$ SD. (C) PPARα agonists potentiate the antiinflammatory effect of DEX in primary murine hepatocytes. Cells were treated for 24 h with either solvent (DMSO), DEX (1 μM), or DEX and WY (10 μM) together. Total RNA was prepared from mouse hepatocytes. RNA concentration and quality were verified using the Agilent 2100 BioAnalyser (Agilent Technologies, Massy, France). Total RNA (1.5 μg) was used to synthesize double-stranded cDNA using Superscript II and DNA Polymerase I (Invitrogen, Eragny, France), and the template for an in vitro transcription reaction was used to synthesize biotin-labeled antisense cRNA (GeneChip Expression 3′-Amplification Reagents for IVT Labeling; Affymetrix, Inc.); 15 μg of labeled cRNA was fragmented (Tris-acetate, KOAc and MgOAc buffer; 94 °C for 35 min), hybridized to the Affymetrix Mouse Genome 430.2 GeneChips and scanned (Affymetrix GeneChip Scanner GCS3000), according to the Affymetrix GeneChip protocol. Very stringent quality verifications at the different steps of the protocol (including total RNA integrity, reverse transcription rate, amplification and cRNA labeling efficiency, hybridization on the chips and quality of the probesets using the intensity signals of housekeeping reference genes) did not lead to the exclusion of samples. Background correction and quantile normalization were performed for the raw microarray data using Bioconductor tools resulting in probesets intensities for each GeneChip. The analysis consisted of comparing expression data from two conditions (DMSO as reference). Ratios were calculated for each probeset, allowing identification of differential gene expression. Statistical analysis was not performed because there was a single Genechip for each condition. The data table represents the mRNA modulation profiles of the reference compounds as compared with the DMSO control. For negative modulation (values <1), the ratio is determined by dividing -1 by the experimental samples over control ratio. Negative values correspond to gene inhibition.

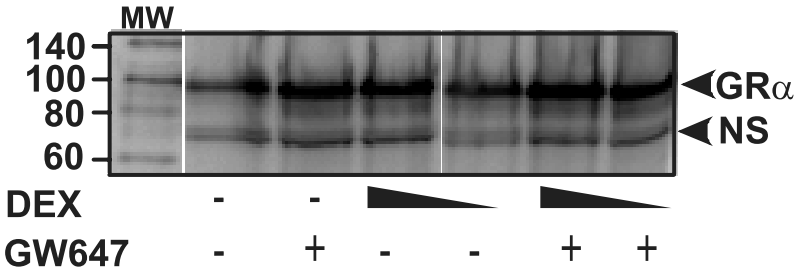

Fig. S2. Activation of PPARα does not affect GRα protein levels. Western blot analysis of a pool of four 24-well plates (from the same transfection and induction set-up as Fig. 2*D*), corresponding to 30 μg of total protein, was performed using an anti-GRα rabbit polyclonal antibody (upper bands, GRα). NS is a nonspecific band that serves as a loading control.

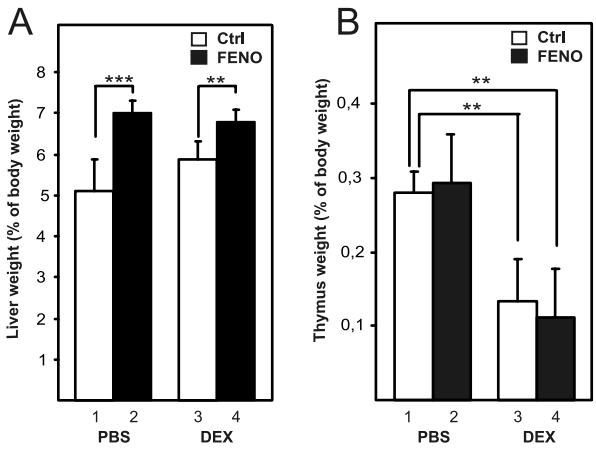

Fig. S3. Activation of GRα does not affect PPARα agonist-induced changes in liver weight, and activation of PPARα does not affect GC-induced changes in thymus weight. Groups of 6 mice per group, randomized according to their weight, were treated with either DEX (10 mg/kg, i.p.) or an equal volume of normal saline, and/or fenofibrate (FENO) (200 mg/kg, gavage) or an equal volume of 0.5% CMC (control) every day for a period of 5 days. Animals were killed, after which liver and thymus were isolated and weighed. (*A*) Liver weight does not differ between FENO and FENO/DEX treatments. FENO-treated mice have a higher liver weight compared with controls ($P < 0.0001$), a known effect of PPARα-mediated hypertrophy and hyperplasia in livers of mice. However, there was no significant change in the liver weights of DEX-treated and FENO/DEX-treated mice compared with controls and FENO alone, respectively. From this result we may conclude that the functional interaction between PPARα and GRα is restricted to specific pathways. (*B*) Thymus weight does not differ between DEX and FENO/DEX treatments. We also measured thymus weight as a marker of GC activity. DEX treatment reduced the weight of the thymus to $<$50% compared with the saline-injected mice ($P < 0.001$). Treatment with FENO did not cause additional effects, suggesting that GC-dependent mechanisms affecting thymus weight are not influenced by PPARα activation, again arguing for a certain degree of specificity in the cross-talk mechanism in analogy to the conclusions made for *A*.

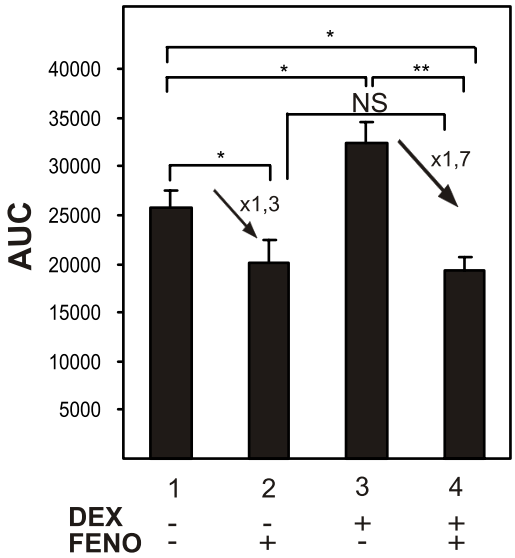

Fig. S4. PPARα activation improves glucose tolerance in a combined high-fat diet and GC-mediated hyperinsulinemic mouse model. Groups of 6 mice per group with an acquired hyperinsulinemia through the intake of a high-fat diet for 7 weeks were daily treated with PBS (control), DEX (2.5 mg/kg), fenofibrate (FF) (200 mg/kg), or DEX/FF combined, for 7 days, after which an i.p. Glc tolerance test (IPGTT) was performed, measuring blood Glc levels before and 15, 30, 45, 60, and 90 min after a Glc injection (see Fig. 5*A* in the main text). The area under the curve (AUC) values were measured and displayed in the graph with the corresponding SD values. Differences between groups were explored via the Mann–Whitney statistical analysis. The AUC values of the IPGTT test (Fig. 5*A*) were measured. The fold change by FF treatment is higher in the presence than in the absence of DEX, i.e., 1.7 versus 1.3, suggesting the existence of an additional cross-talk between PPARα agonists and GCs and indicating that the effect of FF is most likely not dominant to the effect of DEX.

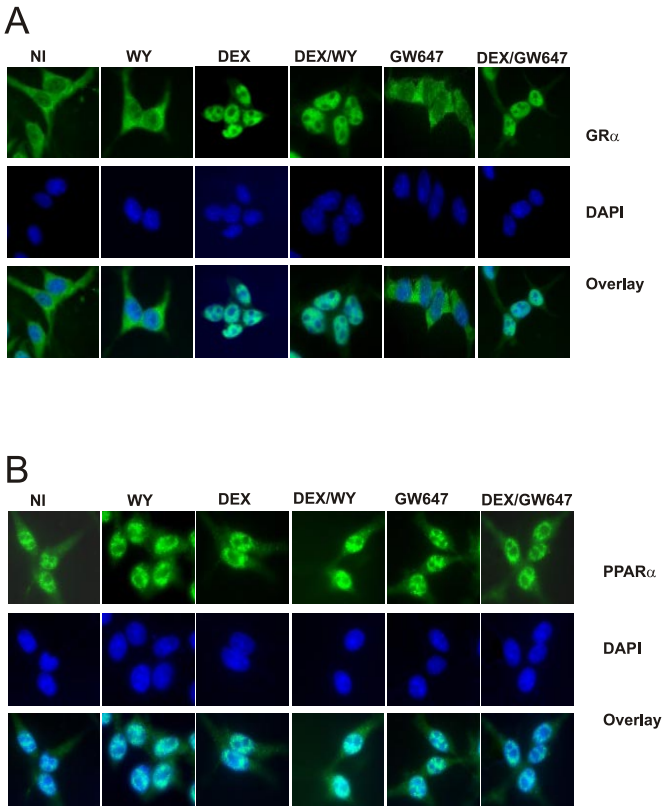

Fig. S5. PPARα agonists do not influence the GC-induced nuclear translocation of GRα, and GC treatment does not affect the subcellular localization of PPARα. After serum starvation in phenol red-free medium for 24 h, BWTG3 cells were treated with solvent (NI) or induced with DEX (1 μM), WY (50 μM), GW647 (500 nM), or various combinations thereof. After fixation, cells were subjected to immunostaining with anti-GR or PPARα, followed by anti-rabbit Alexa Fluor 488 as a secondary Ab. DAPI staining was used to visualize the nuclei. Fixation, permeabilization, and immunostaining procedures with BWTG3 cells were performed as described [De Bosscher K, et al. (2005) *Proc Natl Acad Sci USA* 102:15827–15832]. Images were acquired by using the 63× lens of a Zeiss axiovert 200 microscope and with AxioVision Rel.4.5 software. (*A*) PPARα agonists do not influence the DEX-induced nuclear translocation of GR. Because GRα moves from the cytoplasm to the nucleus upon loading with hormone, we wondered whether activated PPARα would be able to influence the subcellular localization of activated GRα. By means of indirect immunofluorescence, analyzing the subcellular distribution of endogenous GRα protein in BWTG3 hepatocytes, it was clear that in solvent-treated cells GRα is predominantly cytoplasmic, although a certain fraction of GRα appears to be already nuclear. Induction with DEX for 3 h leads to an efficient nuclear translocation of GRα. PPARα ligands do not affect the subcellular localization of GRα. Upon combining DEX and PPARα ligands, PPARα agonists do not influence the DEX-induced nuclear translocation of GR. (*B*) PPARα is localized predominantly in the nucleus, regardless of the presence of PPAR agonists or PPAR agonists combined with DEX. The various treatments did not affect the subcellular localization of PPARα, which is always predominantly nuclear.

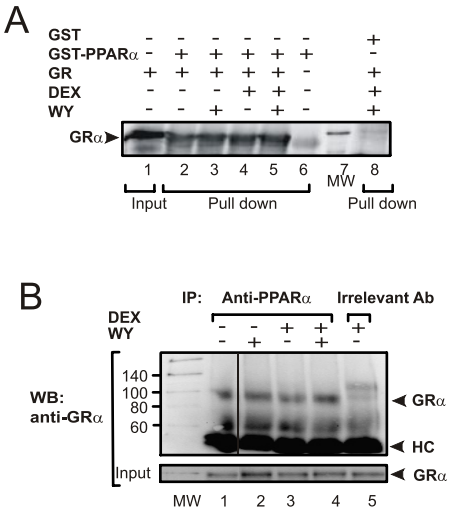

Fig. S6. PPARα can physically interact with GRα. GR proteins were transcribed and translated in vitro by using the TNT T7-coupled reticulocyte lysate system (Promega) according to the manufacturer's instructions. GST pulldown was carried out by incubating the equivalent of 2 μg of GST-PPARα beads with 4 μL of in vitro translated GRα in the presence or absence of WY-14643 (50 μM) and/or DEX (1 μM) in a total volume of 200 μL of incubation buffer [20 mM Tris·HCl (pH 8), 300 mM NaCl, 6 mM $MgCl_2$, 8% (vol/vol) glycerol, 0.05% Nonidet P-40, 0.1% DTT]. The mixture was gently rotated for 2 h at 4 °C. After centrifugation, the beads were washed five times with incubation buffer supplemented with NaCl up to a final concentration of 500 mM, resuspended in 25 μL of 1$\times$ Laemmli buffer, boiled for 3 min, and centrifuged. The supernatant was subjected to Western blot analysis. Membranes were probed by using an anti-GR Ab overnight at 4 °C. Immunoprecipitation assays followed by Western blotting were performed essentially as described [Adcock et al. (1999) *Br J Pharmacol* 127:1003–1011]. (*A*) GST pulldown analysis demonstrates a ligand-independent interaction between PPARα and GRα. To test the possibility that GRα and PPARα could physically interact, we first performed GST pulldown experiments. The figure demonstrates that GRα can specifically interact with PPARα (lanes 2–5) because no binding could be detected in the presence of GST protein alone (lane 8). Although no ligand dependence is apparent, this in vitro result does indicate that both proteins can directly interact. This result was reproduced for three times. In vitro translated GRα protein, using rabbit reticulocyte lysate, was incubated with glutathione–Sepharose 4B beads loaded with GST-PPARα or GST proteins (lanes 2–5 and lane 8, respectively) in the presence or absence of WY (10 μM) and/or DEX (1 μM); bound GRα proteins were eluted and analyzed by SDS/PAGE. Lane 6 contained the rabbit reticulocyte control lysate alone. The membrane was probed with an anti-GR rabbit polyclonal Ab. The result is representative of four independent experiments. (*B*) Endogenous PPARα and GRα interact in a ligand-independent manner. To verify whether the interaction between GRα and PPARα can also occur in cells, we performed a coimmunoprecipitation analysis, with an anti-PPARα Ab, in murine BWTG3 cells. The presence of GRα in the endogenous immune complexes was confirmed by Western blot analysis (lanes 1–4), indicating that PPARα and GRα can also form a protein complex in vivo. Quite unexpectedly, and seemingly in contrast to our analysis of gene expression (Fig. 2), we repeatedly found that PPAR–GR complex formation is ligand-independent in cells and in reconstituted in vitro experiments. The fact that GRα and PPARα can physically interact may nevertheless contribute to the inhibitory effect of activated PPARα on glucocorticoid response element (GRE)-driven gene expression. BWTG3 cells were treated with solvent, DEX (1 μM), WY (10 μM), or a combination of both compounds for 3 h. Immunoprecipitation using an anti-PPARα Ab was followed by Western blot analysis with anti-GR. Lanes 1–4 represent the immunoprecipitation with anti-PPARα in the presence (+) or absence (−) of ligands, as indicated in the figure. An irrelevant Ab was used as a control for specificity. The input represents one-third of the amount used in the assay. The result is a representative of two independent experiments. The displayed bands were blotted onto one single membrane. MW, molecular weight.

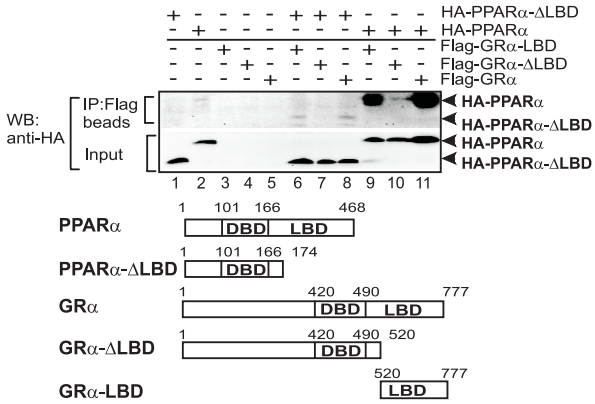

Fig. S7. Domain mapping of the physical interaction between PPARα and GRα. To explore further the determinants of the interaction, we performed domain interaction experiments in the presence of GW647 and DEX. As expected, full-length PPARα efficiently interacts with full-length GRα (lane 11). The ligand-binding domain (LBD) of GRα contributes to the physical interaction because the interaction between full-length PPARα and GR without its LBD (GR$\alpha-\Delta$LBD) is almost completely lost (lane 10) and because the LBD of GRα (GR$\alpha-$LBD) is sufficient to interact with full-length PPARα (lane 9). Notably, the interaction of PPARα without its LBD (PPAR$\alpha-\Delta$LBD) with full-length GRα or GR$\alpha-$LBD is severely compromised (lane 8 and lane 6). A complete loss of interaction is apparent when PPAR$\alpha-\Delta$LBD is combined with GR$\alpha-\Delta$LBD (lane 7), confirming that the LBDs of both receptors are crucial for the physical interaction. Equal amounts of differently tagged receptor variants were transfected in HEK293T cells. Cells were stimulated as indicated in the figure, followed by coimmunoprecipitation analysis of the nuclear fraction by using anti-FLAG beads and immunoblotting with an anti-HA Ab. Input controls were verified by Western blot analysis using anti-FLAG and anti-HA. A representative of two independent experiments is shown. GW647 (500 nM) and DEX (1 μM) was added in every setup containing the respective full-length or deleted receptor plasmids.

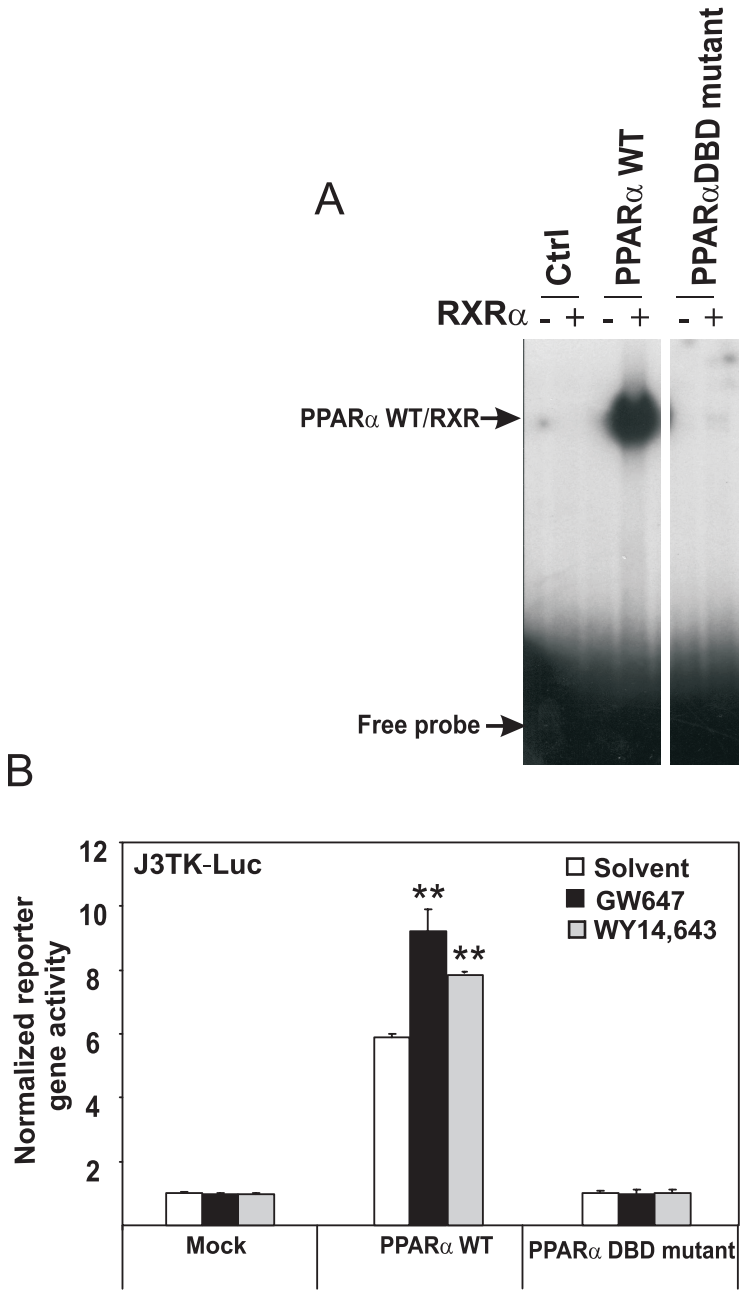

Fig. S8. Characterization of the PPARα-DBD mutant. (*A*) Electrophoretic mobility shift assay of the DR1 consensus was performed, using proteins as indicated in the figure. Mouse PPARα wild type (WT) and the PPARα DBD mutant proteins were obtained from expression vectors by in vitro transcription and translation T3 TNTR-coupled reticulocyte lysate system (Promega). Translation was followed by SDS/PAGE analysis and visualized by immunoblotting using a PPARα-specific antibody (Santa Cruz Biotechnology) to assess the correct size of translated proteins. In vitro translated proteins were preincubated for 10 min at room temperature in a total volume of 20 μL containing 0.5 μg of poly(dI·dC) and 0.5 μg of herring sperm DNA in the following binding buffer: 10 mM Hepes (pH 7.8), 100 mM NaCl, 0.1 mM EDTA, 0.5 mM DTT, 1 mg/mL BSA, and 10% (vol/vol) glycerol. The radiolabeled probes (1×10^5 cpm of ^{32}P-labeled probe) were added, and the binding reaction was incubated for a further 15 min at room temperature. The proteins–DNA complexes were resolved on 6% nondenaturating PAGE in a 0.5% Tris–borate–EDTA running buffer at room temperature and visualized after autoradiography. Only PPARα WT, but not the triple-point mutant, can bind DR1, in the presence of retinoic acid receptor (RXR). Human hydroxymethyl-glutaryl-CoA synthase (HMG-CoA synthase), human CPT-1, and ACO PPREs gave similar results. (*B*) The PPARα DBD mutant does not support transactivation of a PPRE-driven reporter gene. Equal amounts of the corresponding empty vector, PPARα WT or the PPARα DBD mutant were transfected together with J3TK-luc (a PPRE-driven reporter gene) and the β-galactosidase expressing plasmid in HEK293T cells. Cells were stimulated for 8 h with solvent, WY (50 μM), or GW647 (500 nM). Cell lysates were assayed for luc activities and normalized for β-gal activities. Promoter activities are expressed as relative induction factor, i.e., the ratio of expression levels of induced versus the noninduced (mock) condition.